Fuel 276 (2020) 118008

Contents lists available at ScienceDirect

Fuel

journal homepage: www.elsevier.com/locate/fuel

Full Length Article

Comparative studies on the ignition characteristics of diisobutylene isomers and *iso*-octane by using a rapid compression machine

Yingtao Wu, Meng Yang, Xiaoxin Yao, Yang Liu, Chenglong Tang*

State Key Laboratory of Multiphase Flow in Power Engineering, Xi'an Jiaotong University, Xi'an 710049, China

ARTICLE INFO

Keywords:
Iso-octane
DIB-1
DIB-2
Rapid compression machine
IDTs

ABSTRACT

In this work, we have compared the auto-ignition behaviors of 2,4,4-trimethyl-1-pentene (DIB-1) and 2,4,4-trimethyl-2-pentene (DIB-2), and *iso*-octane in the low to intermediate temperature range (660–950 K) over various equivalence ratios at 20 and 30 bar using a rapid compression machine. Results show that *iso*-octane exhibits the expected negative temperature coefficient (NTC) behavior and the highest reactivity (lowest ignition delay times, IDTs) in the low temperature region. Both DIB-1 and DIB-2 show less low-temperature reactivities and quasi-Arrhenius temperature dependence of the IDTs were observed at all test conditions. Due to the similarity of the molecular structure of DIB-1, DIB-2 and *iso*-octane, the effects of the unsaturated bond and its position are assessed and compared with that for linear alkenes. The IDT data of DIB-1, DIB-2 and *iso*-octane were then used to validate several recently developed kinetic models. Results show that the performances of the *iso*-octane models are generally good, while model performance for predictions of IDTs for DIB needs to be improved especially at low temperatures. Finally, kinetic analyses explained the reactivity difference caused by double bond and its position, based on which further model optimization suggestions are proposed.

1. Introduction

The development and design of modern engine and burner rely more and more on combustion simulation, which motivates the study on fuel oxidation kinetics. However, because of the complexity of the practical fuel compositions, a complete description of combustion chemistry for practical engine fuels coupled with the fluid dynamics is still beyond the present computational capability and the current understanding on combustion chemistry. Consequently, surrogates [1,2] containing a limited number of components but with representative functional groups are typically selected for reproduction of the physical property and the combustion parameters of the practical fuels.

Commercial gasoline contains linear and branched alkanes, cycloalkanes, alkenes and aromatics. Its surrogate components [2] have been developed from the unitary of *iso*-octane to the binary of primary reference fuels (PRF) [2–9], which contains n-heptane and *iso*-octane, then to the ternary of toluene primary reference fuels (TPRF) [10] with the addition of toluene which represents the aromatics, and recently more multi-component surrogate models have been developed [11]. With the increment of the components number, each main class of the hydrocarbon in the real fuels can be represented in the surrogates, and thus more reliable approximation can be achieved. However, the development of the surrogate model has also increased the complexity of the chemical reaction system. The mechanism of each component should be well characterized over a wide range of conditions, so that the fundamental combustion parameters such as the laminar flame speed, the ignition delay times (IDTs) and the intermediate species mole fraction profiles can be better predicted. *Iso*-Octane, representing the branched alkanes in the gasoline, has been thoroughly studied both experimentally and theoretically over the past decades [6,9]. Since most alkenes in the commercial gasoline are branched, diisobutylene (DIB) has been selected to represent the branched alkenes in the surrogate model [12] and increase the octane number of the fuel mixtures due to the existence of the double bond [13]. However, very limited auto-ignition data have been reported and the kinetic models of DIB are not sufficiently validated, especially in low temperature range.

Metcalfe et al. [14] measured the IDTs of the two neat DIB isomers, i.e. 2,4,4-trimethyl-1-pentene (DIB-1) and 2,4,4-trimethyl-2-pentene (DIB-2), and their blends in a shock tube, at pressures of 1 and 4 atm, and in the temperature range between 1200 and 1550 K. They found that DIB-2 has a significantly shorter IDTs than DIB-1 under the researched conditions. Furthermore, a kinetic model was carried out based on the *iso*-octane mechanism of Curran et al. [9], and it yielded a good prediction of the IDTs. Mittal et al. [15] investigated the auto-ignition behaviors of DIB-1 and its blends with toluene in a rapid compression machine (RCM) at pressures varying from 15 to 45 bar and

* Corresponding author.
E-mail address: chenglongtang@mail.xjtu.edu.cn (C. Tang).

https://doi.org/10.1016/j.fuel.2020.118008
Received 20 April 2020; Received in revised form 29 April 2020; Accepted 1 May 2020
Available online 11 May 2020
0016-2361/

in low to intermediate temperature range. Result shows that DIB-1 has shorter IDTs than *iso*-octane in higher temperature region and longer IDTs at temperatures lower than 820 K, and the addition of DIB-1 has greatly increased the reactivity of the toluene oxidation. More recently, the high-temperature IDTs, laminar flame speeds, and oxidation species profiles of DIB-1 by using a shock tube, combustion bomb and jet-stirred reactor respectively under various conditions have been provided [16–19]. High-level quantum calculations were performed in their model optimization for some important reactions and the modified model shows fairly good predictions at their researched conditions. Based on the DIB mechanism of Metcalfe et al. [14], various DIB-containing gasoline surrogate models [10,12,20–24] were developed with only limited modification to the DIB-1 high-temperature sub-mechanism.

Although researches of the DIB-containing surrogate have been widely conducted, validation of the DIB-sub mechanism has only been tested against the high-temperature ignition delay data, as in Ref. [14]. Except for work of Mittal et al. [15] which involves three RCM data sets on DIB-1, the limited experimental data of pure DIB is mainly in high temperature range, while the low temperature oxidation data of DIB is yet not been sufficiently provided. Low temperature combustion is more relevant to the engine working conditions and fuel oxidation process is more complicated and fuel depended. Therefore, the first objective of this work is to provide IDTs of DIB-1 and DIB-2 over the temperature range of 660–950 K, equivalence ratio from 0.5 to 1.5 and at two pressures by using an RCM.

In addition, DIB isomers are important intermediates in the oxidation of *iso*-octane and they also have very similar molecular structures with *iso*-octane. As such, studies on the oxidation scheme of DIB not only favor our understanding on combustion chemistry of *iso*-octane and the gasoline surrogate, but also shed light on the double bond kinetics. Previous works [25,26] have investigated the double bond and its position influence on the overall reactivity at low temperatures for large linear alkenes, we will then compare the ignition data of DIB-1, DIB-2 and *iso*-octane to assess if the reported double bond influence for large linear alkene is still valid for branched alkenes.

Finally, since the Metcalfe model [14] has been embedded and modified in many literature models, our third objective is then to validate these models against our newly measured data and kinetically reveal the low temperature oxidation channels in the oxidations of DIB isomers.

2. Methodology

The IDTs of DIB-1 (Alfa, 98%), DIB-2 (TCI, 98%) and *iso*-octane (TCI, 99%) were collected using the RCM in Xian Jiaotong University. Details of this facility description can be found in Ref. [27], including the creviced piston design and validation of the measured IDTs. Briefly, the RCM contains six sections, as shown in Fig. 1, the high pressure tank, the driving chamber, the hydraulic chamber, the compression chamber, the combustion chamber, and the control and data acquisition system. A creviced piston is employed to ensure the temperature homogeneity inside the combustion chamber. The length of the combustion chamber is adjustable to realize different compression ratios. The reactive and corresponding non-reactive (replacing O_2 with N_2 in the mixtures) gas mixtures were separately prepared in a stainless-steel tank according to the partial pressure of each component for the desired mixtures. The partial pressures of the fuels (DIB-1, DIB-2 and *iso*-octane) were kept below at least 1/2 of their saturated vapor pressures to avoid condensation. Pressure and temperature at the end of compression (p_c, T_c) are used as the physical conditions for the IDT characterization. The pressure profiles were measured by a piezoelectric pressure transducer (Kistler 6125C), while the temperature was calculated based on the adiabatic core hypothesis [28], as shown in Eq. (1).

$$\int_{T_0}^{T_c} \frac{\gamma}{\gamma - 1}\frac{dT}{T} = \ln\left(\frac{P_c}{P_0}\right) \tag{1}$$

where T_0 is the initial temperature, P_0 is the initial pressure, γ is the temperature-dependent specific heat ratio of the gas mixture. The thermodynamic data used to calculate γ is adopted from the DIB model of Metcalfe et al. [14] for DIB-1 and DIB-2, and the *iso*-octane model of Mehl et al. [29,30] for *iso*-octane, in which the thermodynamic has been updated based on the group additivity method proposed by Benson [31].

Fig. 2 shows the typical pressure evolution histories for the three fuels studied in this work. The instant of the maximum pressure value before chemical heat release is selected as time zero. An obvious two staged ignition behavior was observed for *iso*-octane, as represented by twice rises on the pressure evolution profiles after the end of compression. The IDTs are determined from the pressure histories: the first staged (1st) and total IDTs are respectively defined as the time intervals between time zero and the steepest pressure rise at the two ignition onsets. For DIB-1 and DIB-2, the pressure traces show only single staged ignition. The uncertainty in plotting IDTs mainly comes from measurements of temperature and pressure. The uncertainty in pressure is due to uncertainty in initial pressure measurement, pressure transducer, and charge amplifier. The uncertainty in temperature comes from uncertainty in initial temperature measurement, and the uncertainty in pressure measurement. Therefore, uncertainty of the current experimental study is given in two ways: uncertainty in T_c in the horizontal direction and repeatability in the vertical direction [32,33]. By using the independent parameters methodology [32], uncertainty of T_c for each data point is calculated, as provided in Supplementary material. Generally, the uncertainty of T_c is less than 8 K. The repeatability of current measurements is generally within 15% which has been shown as the error bars in the plots. For reactive measurements, the pressure traces were carefully examined to insure there is no significant pre-ignition heat release [34] before autoignition.

Simulations of the autoignition are conducted using CHEMKIN Pro 18.2 software [35] adopting non-reactive volume profiles [36,37]. The instant of the maximum pressure rise rate (dp/dt) is recognized as the ignition onset. The kinetic models simulated in this study include: (a) DIB model of Metcalfe et al. [14]; (b) the *iso*-octane model of Atef et al. [6]; and (c) *iso*-octane model of Mehl et al. [29,30]. Metcalfe model, with 897 species and 3783 reactions, was developed based on the *iso*-octane model of Curran et al. [9], and has been validated against high-temperature IDTs. Atef model was built in a hierarchical way in which the C_0–C_4 base model is from AramcoMech 2.0 [38], the C_5–C_7 sub-models are from LLNL's gasoline surrogate model [39] and the DIB chemistry in the C_8 sub-model is from Metcalfe model [14]. Atef model has 2167 species, 9230 reactions and has been validated against shock tube IDT, jet stirred reactor oxidation speciation, laminar flame speed, RCM autoignition and shock tube pyrolysis. Mehl model was also developed based on the *iso*-octane model of Curran et al. [9] with 874 species and 3796 reactions and it has been validated against both shock tube and RCM IDTs. Since model (b) has included model (a) as a sub-mechanism, the former two models were validated against the IDTs of DIB-1 and DIB-2. While, model (b) and (c) were used in the simulations of *iso*-octane autoignition.

3. Results and discussion

3.1. Measured IDTs

The IDTs for the stoichiometric fuel (DIB-1, DIB-2 and *iso*-octane)/O_2/Ar mixtures at pressures of 20 and 30 bar were measured over the temperature range of 660–950 K. In addition, the equivalence ratio (ϕ) effect on the low temperature reactivities was also checked for DIB-1 and DIB-2 mixtures at ϕ = 0.5 and 1.5, 20 and 30 bar. Since DIB is a

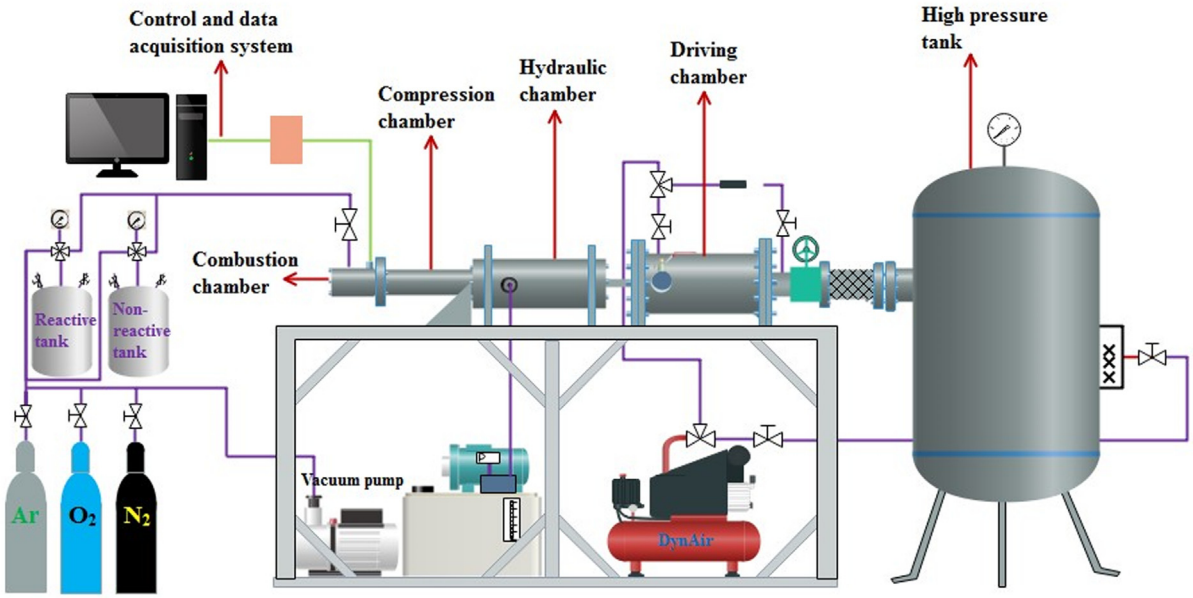

Fig. 1. Scheme of the RCM in Xian Jiaotong University.

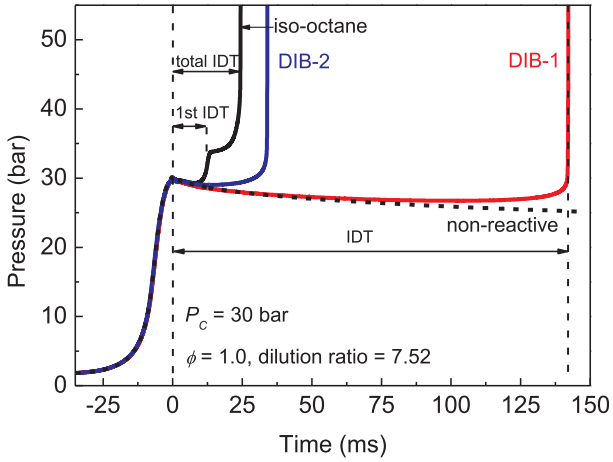

Fig. 2. Typical pressure traces for the autoignition of DIB-1, DIB-2 and *iso*-octane.

Table 1
Mixture fractions.

Fuel	O_2	Ar
0.93% *iso*-octane	11.63%	87.44%
0.97% DIB-1	11.62%	87.41%
0.49% DIB-1	11.68%	87.83%
1.92% DIB-1	11.51%	86.57%
0.97% DIB-2	11.62%	87.41%
0.49% DIB-2	11.68%	87.83%
1.92% DIB-2	11.51%	86.57%
0.73%DIB-1/0.24%DIB-2	11.62%	87.41%

blend of DIB-1 and DIB-2 at a ratio of about 3:1, the autoignition characteristics of a DIB blend were also measured in this study and compared with that of the pure DIB isomers. The components concentrations of each mixture are given in Table 1 and the details of all the measured IDTs are provided in the Supplemental material.

3.1.1. IDTs of DIB-1 and DIB-2

Fig. 3 shows the effect of equivalence ratio on the IDTs of DIB-1 and DIB-2/O_2/Ar mixtures at 30 and 20 bar. The IDTs decrease with the increment of ϕ, indicating an enhanced reactivity for richer mixture. Distinct from large linear alkenes, hexenes [40] and heptenes [25] for example, DIB isomers did not show NTC nor two staged behaviors and their low-temperature reactivities are rather slow under the studied conditions. Quasi-Arrhenius temperature dependence was observed for the IDTs of DIB-1 and DIB-2 at different conditions. One interesting phenomenon for DIB-1 mixtures is that the fitted overall activation energies are slightly decreased for richer fuel mixtures indicating more profound low-temperature reactivities. At 30 bar, ϕ = 1.5, the IDTs of DIB-1 mixture seems to reach the high temperature limit of a mild NTC region, however, further measurements at lower temperatures (scatters with crossline) have exceeded the reliability range of the RCM (< 200 ms) [33] due to the decaying of the "adiabatic core" [27]. As for the pressure effect, IDTs at higher pressures are generally shorter as expected and thus are not directly compared here in the plots. Although higher pressure has improved the reactivity of both fuels, the autoignition of DIB-1 seems to be more sensitive to the pressure change than DIB-2. For p_c = 20 bar, as shown in the Fig. 3(b), the low temperature limit (800 K) at which ignition can be measured by this RCM is much higher than that at 30 bar (700 K), and the IDTs for different equivalence ratios are very closed especially at high temperatures.

3.1.2. IDTs of DIB blend

The IDTs of DIB blend (DIB-1:DIB-2 = 3:1) are compared with that of DIB-1 and DIB-2, as shown in Fig. 4. DIB-2 exhibits the highest reactivity under the studied conditions while DIB-1 shows the slowest autoignitions. The IDTs of DIB blend are in the middle between that of DIB-1 and DIB-2. By doing linear fit of the measured IDTs, as shown by the solid lines in Fig. 4, the overall activation energies of the DIB-1, DIB-2 and blend mixtures are respectively 18.80, 12.16 and 17.18 kcal/mol. Noting that the reactivities of DIB-1 and blend are very similar, it is thus reasonable to use DIB-1 to approximately represent DIB in the surrogate model studies. Besides, the logarithm values of the blend' IDTs (τ) are very close to a linear relationship with the proportion of DIB-1 and DIB-2 not only in our measurements but also in the shock tube study of Metcalfe et al. [14], as shown by the dash lines calculated using Eq. (2).

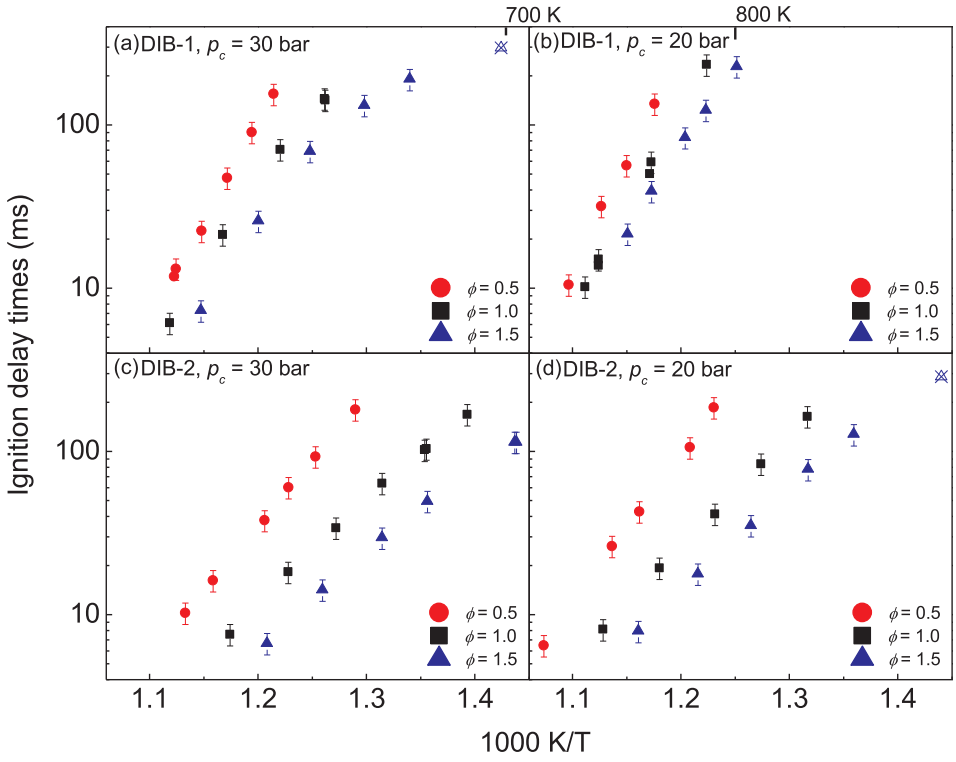

Fig. 3. The measured IDTs of DIB-1 and DIB-2: (a) DIB-1, p_c = 30 bar; (b) DIB-1, p_c = 20 bar; (c) DIB-2, p_c = 30 bar; (d) DIB-2, p_c = 20 bar, at different equivalence ratios.

$$log\tau = \frac{[DIB-1]}{[DIB-1]+[DIB-2]} log\tau_{DIB-1} + \frac{[DIB-2]}{[DIB-1]+[DIB-2]} log\tau_{DIB-2} \quad (2)$$

The calculated values are slightly higher than the fitted ones, yet, they are within 15% errors. This rule of the blending effect on IDTs, however, needs further validation against more IDT data of DIB-1 and DIB-2 at other blending ratios.

3.1.3. Reactivities comparison among DIB-1, DIB-2 and iso-octane

Direct comparisons among the IDTs of stoichiometric DIB-1, DIB-2 and *iso*-octane mixtures at 30 and 20 bar are presented in Fig. 5 to access the effect of double bond. Generally, in temperature range between 660 and 950 K, only the *iso*-octane exhibits an obvious NTC behavior and two staged ignitions which are both reported in the plots. Except for the NTC behavior of the total IDTs, the 1st IDTs of the *iso*-octane mixture also show an NTC trend at 20 bar, yet not observed at 30 bar. The NTC temperature range for the total IDTs of *iso*-octane mixture at 30 bar is 710–820 K and moves to a lower temperature range 690–810 K at 20 bar. The NTC behaviors of *iso*-octane have also caused the changes of the relative reactivities compared with DIB-1 and DIB-2. Below a temperature in the NTC region (760/750 K for 30 and 20 bar respectively), where *iso*-octane has exhibited two staged ignitions, *iso*-octane has the lowest IDTs among these three fuels indicating that the unsaturated bond in the alkyl chain significantly reduced the overall reactivity in this temperature range. However, as temperature rises above 760/750 K, the 1st stage ignition due to the cool flame [41] of *iso*-octane vanishes, and autoignitions of DIB-2 become the fastest in these three fuels. As temperature exceeds the upper limit of the NTC region of *iso*-octane (820/810 K), the DIB-1 becomes more reactive than *iso*-octane, yet always less reactive than DIB-2 under the present conditions.

The reverse of the relative fuel reactivities indicates that the double bond in the *iso*-octane molecular structure has played an opposite role in promoting the reactions at high and low temperatures. At low temperatures, the reactivities of the alkane systems are mainly promoted by the chain branching reactions of the O_2 addition to fuel-derived radicals (R) followed by internal isomerization and decomposition reactions [9,42]. Compared with alkanes, 1) inducing C=C bond in the molecular will weak the C–O_2 bond at the allylic sites, resulting in inhibition of the subsequent isomerization reactions [43] and reducing the low-temperature reactivity; 2) C=C bond is an obstacle for the isomerization reactions: ROȮ to QOOH, and thus inhibits the low-temperature chain branching reactions. 3) Although reducing the bond dissociation energy (BDE) of the C–H at the allylic sites induced by C=C bond favors the H-abstraction reactions, the products are resonantly stabilized radicals which will inhibit the subsequent reactions and thus slow down the system. 4) Inducing C=C bond in the molecular allows the addition of O, OH, H and HO_2 radicals, however, the following reactions of these products [44] are chain propagations which will compete with the low-temperature chain branching reactions and thus slow down the overall reaction rate. The above reasons not only explain why DIB isomers are less reactive than *iso*-octane at low temperatures in this study but can also apply to the reactivity comparisons of the linear structured saturated/unsaturated fuels [25].

At high temperatures, unimolecular decomposition reactions are more favoured to happen and the C–C cleavage at the allylic sites tends to occur due to its weakest BDE, which promotes the reactivity of the system. Besides, inducing C=C bond also increases the reaction rate of the H-abstractions at the allylic sites and accelerate the oxidation initialization. Although the above channels still form resonantly stabilized products, these products can easily undergo C–C cleavage at high temperatures and thus will not inhibit the reactivities. This then explains the reason why DIB isomers are more reactive than *iso*-octane at high temperatures. linear structured saturated/unsaturated fuels [25] comparisons have also shared the same rules in the oxidation.

The comparison of the IDTs of DIB-1 and DIB-2 also reveals the effect of the double bond position in the branched molecular. As shown in Fig. 5, the IDTs of DIB-1 decrease faster with larger activation energy

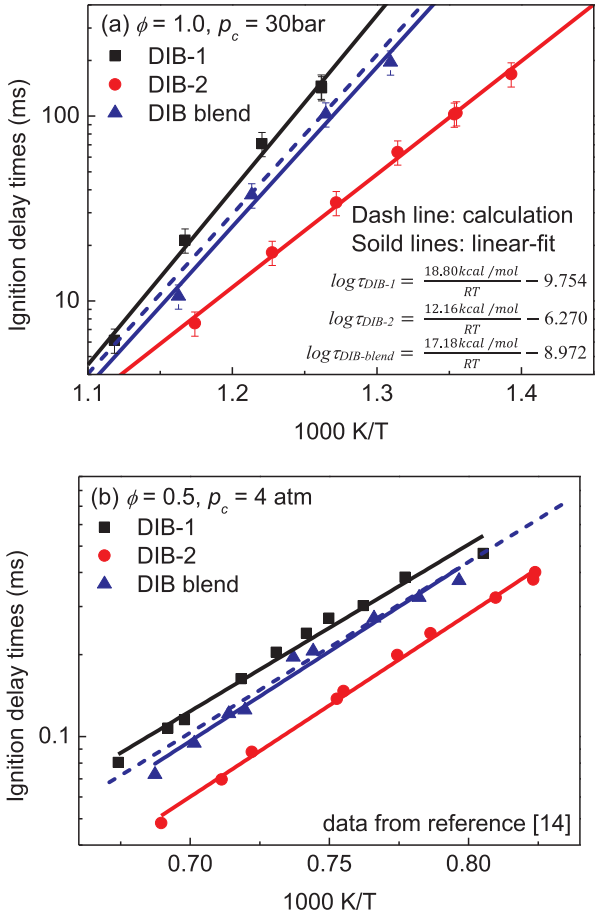

Fig. 4. IDTs of stoichiometric DIB-1, DIB-2 and blend mixtures at 30 bar; Solid lines are the linear-fit lines of the measured data and dash line is the calculation result using Eq. (2).

compared with that of DIB-2 and their IDTs are becoming much closer as the temperature increases, indicating the moderated effect of double bond position at higher temperatures. Limited by the time scale [33] of the RCM measurement, IDTs in the higher temperature range cannot be measured in this study. Literature study [14] using shock tube has shown that DIB-2 is also more reactive than DIB-1 in the temperature range of 1200–1490 K at 4 atm.

The double bond position effects on DIB isomers are different from that on large linear alkenes, hexenes [26,45] and heptenes [25] from example, in which the 1-alkenes are more reactive at low temperatures while less reactive at high temperatures. This is because at low temperatures, the reactivity is mainly dominated by the typical alkane-like reactions of the alkyl chain. As for linear akenes, 1-alkenes have the longest alkyl chains and thus behave more low-temperature reactivities. For DIB isomers, the remain alkyl chains (isopentyl/isobutyl) are highly branched and do not favor the low-temperature chain branching reactions. Therefore, the reactivities of DIB isomers are mainly controlled by the double bond, of which the reactivities are dependent on the number of allylic C–C/C–H bonds and the ability to add O_2 and HO_2 [26]. DIB-2 has more allylic sites than DIB-1, hence at low temperatures, it can add more O_2 or HO_2, while at high temperatures it favours more C–C/C–H cleavages, and thus it is more reactive. However, the autoignition characteristics of DIB isomers in the intermediate temperature range of 910–1200 K are still unknow which requires further experimental work.

3.2. Model validations and discussion

3.2.1. Validations of the iso-octane models

As one of the primary reference fuels, *iso*-octane has seen extensive kinetic modelling research. Among them, the model developed by Curran et al. [9] has been proved to be very successful in predicting the fuel autoignitions. Based on the model of Curran et al. [9], Mehl et al. [2] further optimized the *iso*-octane model in the work of the gasoline surrogate study. The Mehl model [2] was then used here to simulate the IDTs measured in the present study and compared with the most recent *iso*-octane model from Atef et al. [6].

Comparisons on the IDTs predictions using Mehl model and Atef model are shown in Fig. 6. At higher pressure, p_c = 30 bar, both models have well captured the NTC trend and two-stage ignition behaviors. Below the lower limit of the NTC region, the simulation results from both models agree well with the measured 1st and total IDTs. In the NTC region, the model predictions begin to show discrepancies with the experimental data, and both models can only predict well parts of the IDTs. At higher temperatures outside the NTC region, Mehl model has shown very good agreement with the experimental measurements while Atef model has underpredicted the IDTs. Model comparison at 20 bar

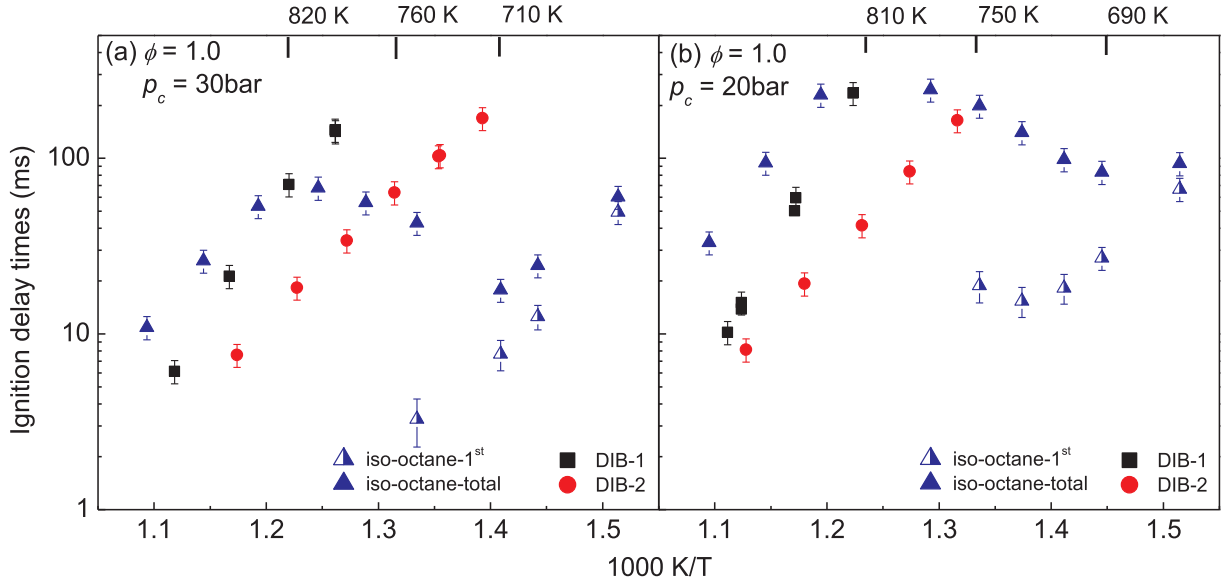

Fig. 5. The IDTs of the stoichiometric mixtures of DIB-1, DIB-2 and *iso*-octane at pressures of 30 and 20 bar.

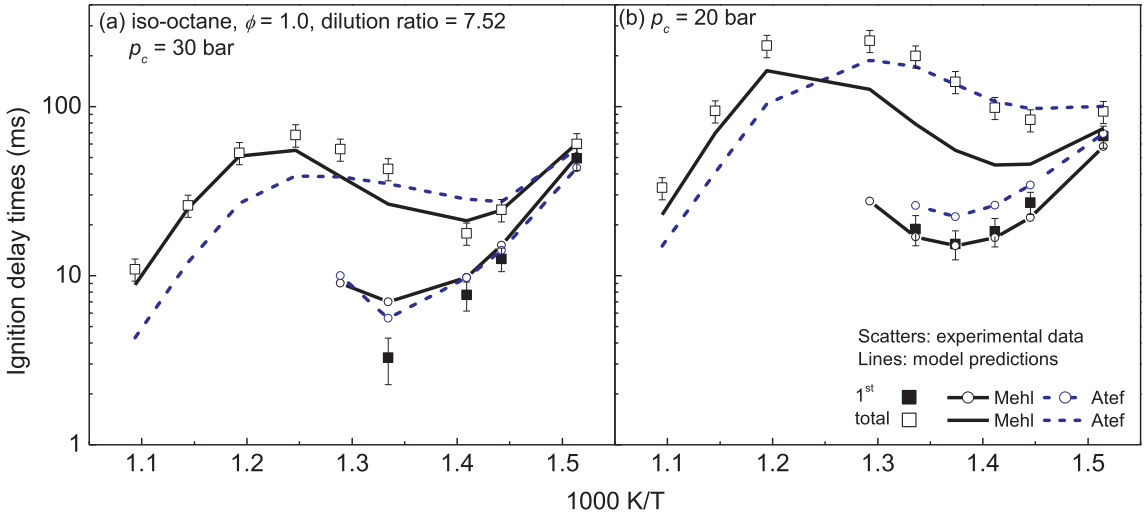

Fig. 6. The IDTs of *iso*-octane and model predictions using Mehl model [2] and Atef model [6] at (a) 30 and (b) 20 bar.

shows similar pattern: compared with Atef model, Mehl model predicts higher reactivities in lower temperature region and lower reactivities in higher temperature region. Besides, both models have well captured the NTC behavior of the 1st IDTs of *iso*-octane at 20 bar, and the predictions from Mehl model agree better with the measurements. For the total IDTs at 20 bar, Atef model has well captured the data in the lower temperature and NTC region, while Mehl model shows underpredicted IDTs especially in the NTC region.

3.2.2. Validations of the DIB models

The model predictions on the IDTs of DIB-1 using Atef model and Metcalfe model are shown as Fig. 7. Generally, Atef model shows better performance than Metcalfe model which overpredicted the reactivities under all conditions. The agreement between the predictions of Atef model and the experimental data is very good at high temperatures yet shows larger discrepancies as temperature decreases. For the IDTs predictions of DIB-2, as shown in Fig. 8, Atef model shows very good performance except for that at some high temperatures of the fuel lean mixture and low temperatures of the fuel rich mixture. The performance of Metcalfe model for DIB-2 is generally better than that for DIB-1, which generates slightly higher predictions for fuel lean mixture and lower predictions for stoichiometric and fuel rich mixtures compared

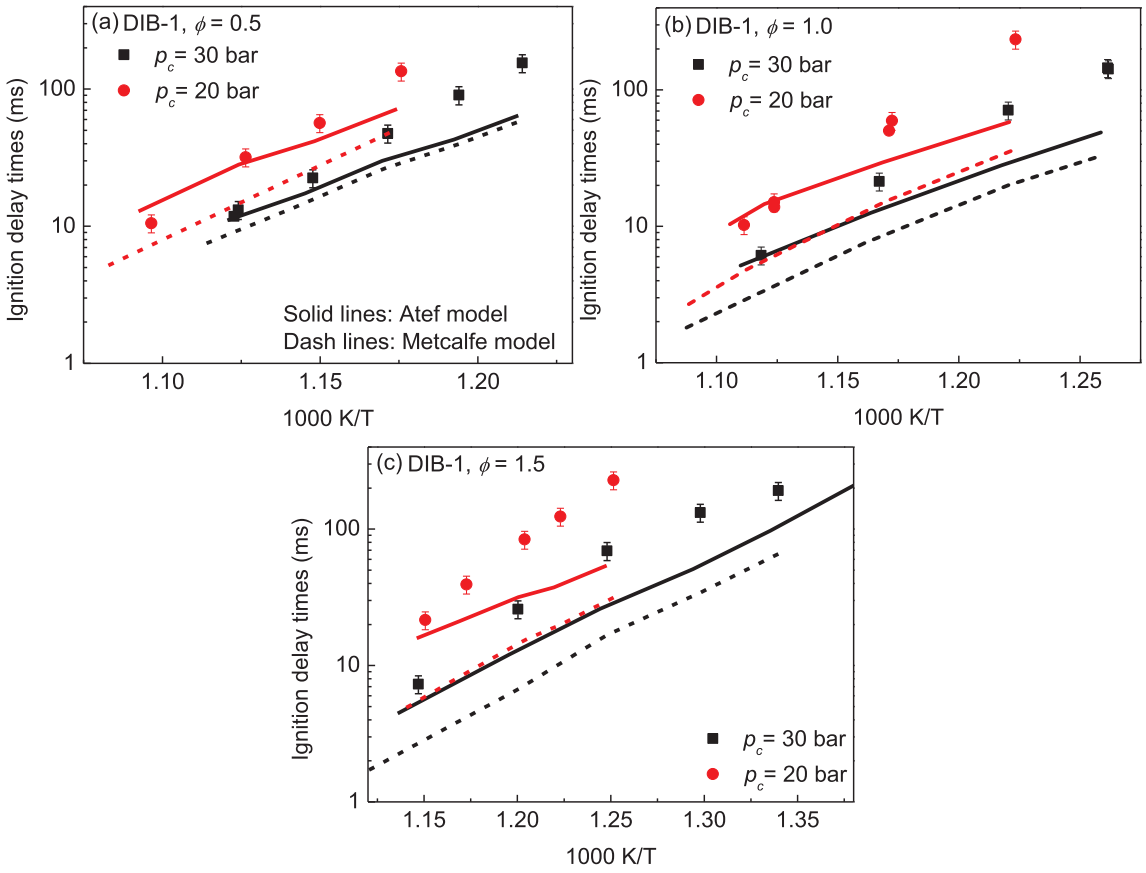

Fig. 7. Comparisons on the model predictions of the IDTs of DIB-1 using Atef model [6] and Metcalfe model [14].

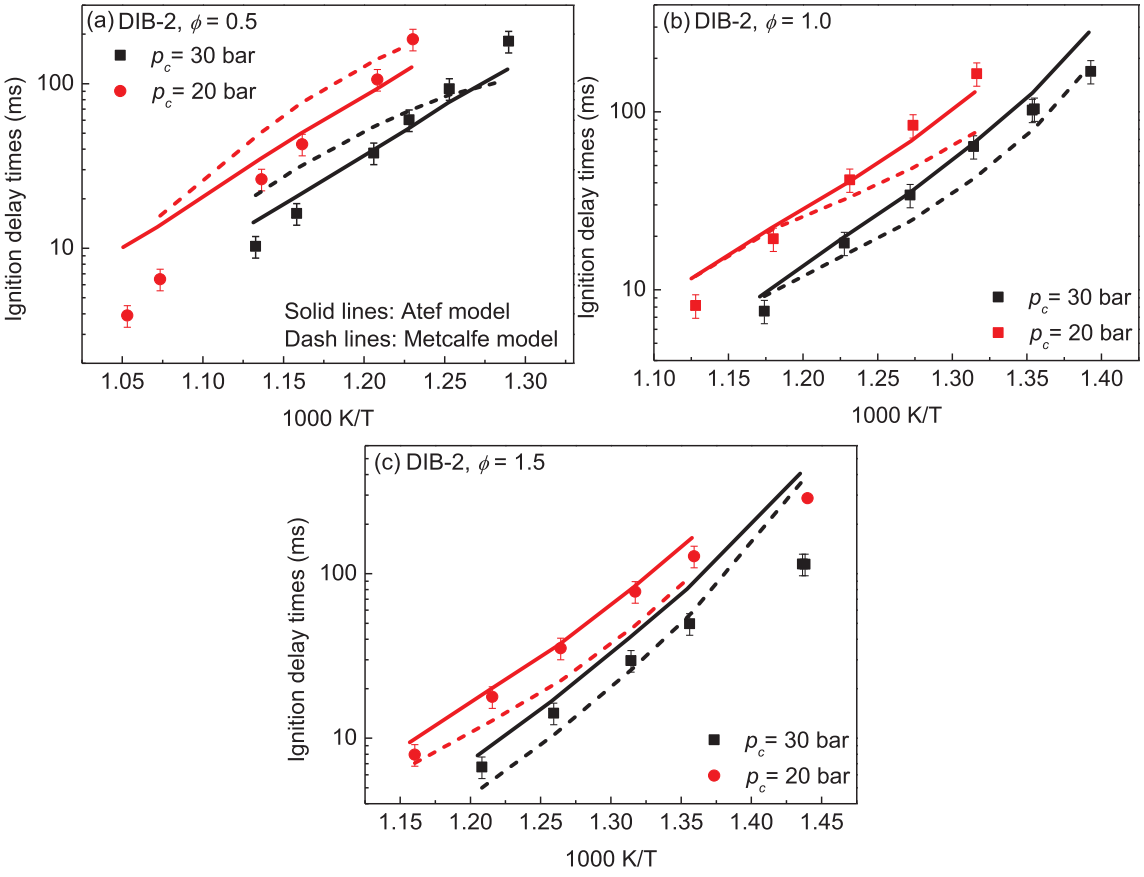

Fig. 8. Comparisons on the model predictions of the IDTs of DIB-2 using Atef model [6] and Metcalfe model [14].

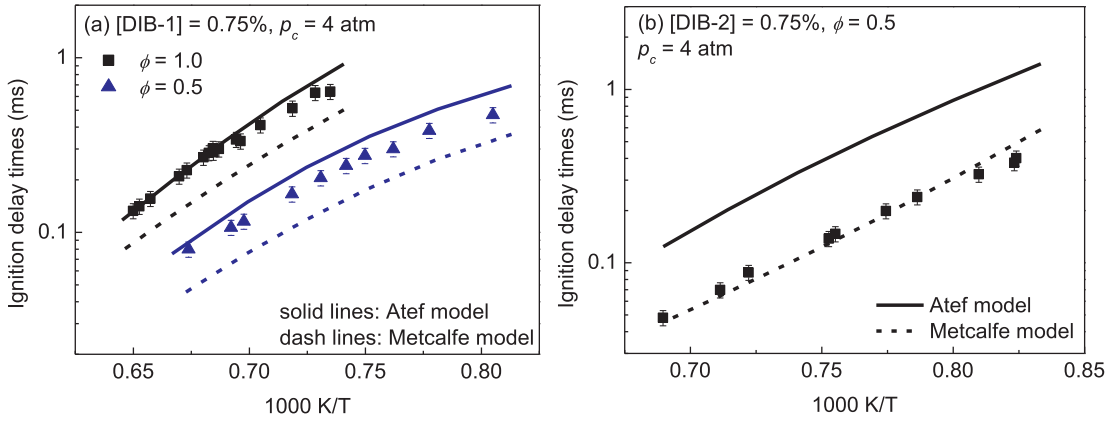

Fig. 9. Comparisons on the model predictions of the high-temperature IDTs of DIB isomers [14] using Atef model [6] and Metcalfe model [14].

with Atef model.

The model performances for high-temperature IDTs of DIB isomers are also assessed by using the shock tube data from reference [14]. As shown in Fig. 9, the Atef model shows very good predictions for the IDTs of DIB-1 at high temperatures (1220–1530 K) while the Metcalfe model overpredicts the reactivities at the studied conditions. For the IDTs of DIB-2, the Metcalfe model predicts the IDTs very well while the Atef model underestimates the reactivities.

Noting that the DIB sub-mechanism in the Atef model is also from Metcalfe model, the improved performance should be attributed to the updated C1–C4 base model and more detail C5–C7 models from the LLNL's gasoline surrogate mechanism [2]. The Metcalfe model was only validated against shock tube IDTs at high temperatures, and typical low-temperature reactions, such as the chain branching reactions of O_2 addition to fuel derived radicals and the following isomerization reactions, are missing in the mechanism. Due to the highly branched molecular structures of DIB, the low-temperature chain branching reactions do not play important roles in determining the reactivities under the studied conditions. Therefore, the Atef model still predict the autoignitions of DIB isomers in a reasonable level especially for DIB-2 whose low-temperature reactions are even less important.

3.2.3. *Kinetic analyses and model discussion*

Since the *iso*-octane model of Atef et al. [6] has contained the sub-models of DIB isomers and it predicts the autoignitions of DIB isomers in a reasonable level, we then have used Atef model in the kinetic analyses to compare the reaction pathways of DIB isomers with *iso*-octane and probe the roles of DIB isomers in the *iso*-octane oxidation.

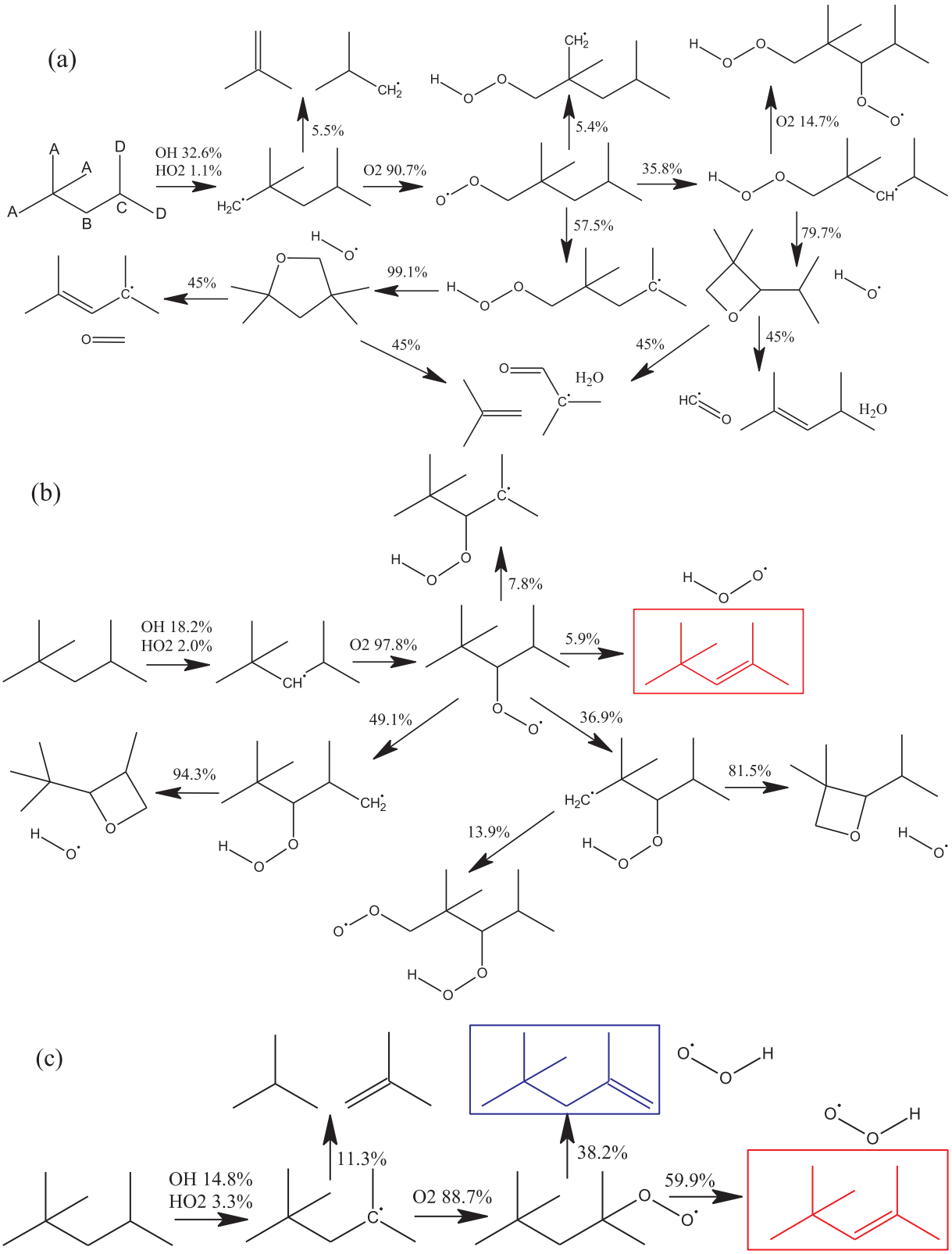

Fig. 10. Reaction flux analysis of *iso*-octane at fuel consumption rate of 20%, 30 bar, 800 K.

The reaction flux analysis of *iso*-octane was conducted at 30 bar, 800 K and fuel consumption rate of 20% [6] where a complete oxidation scheme can be presented, as shown in Fig. 9. The percentage in the figure refers to the relative rate of production (ROP) of a certain species. Noting that 800 K refers to the temperature where *iso*-octane reaches the higher limit of the NTC region and both DIB isomers show moderate reactivities. The consumptions of *iso*-octane are mainly through H-abstractions by OH radicals while the contribution of HO_2 and other radicals is rather less. The most important consumption channel is through the O_2 addition on AC_8H_{17}, as shown in Fig. 9(a). In the $AC_8H_{17}O_2$ isomerization, H-shit from A sites counts for only 5.4% while that from B (6-member) and C (7-member) sites counts a lot more

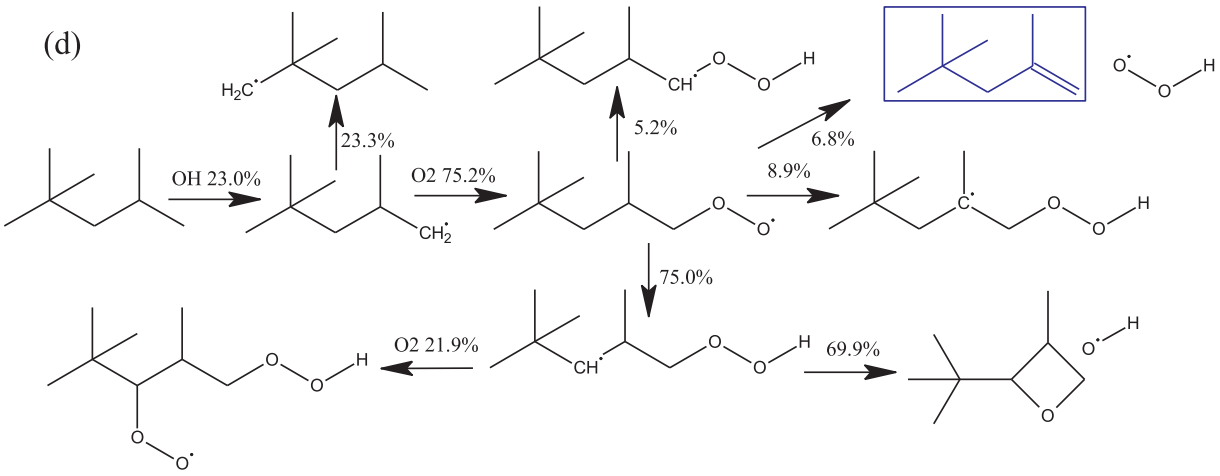

Fig. 10. (*continued*)

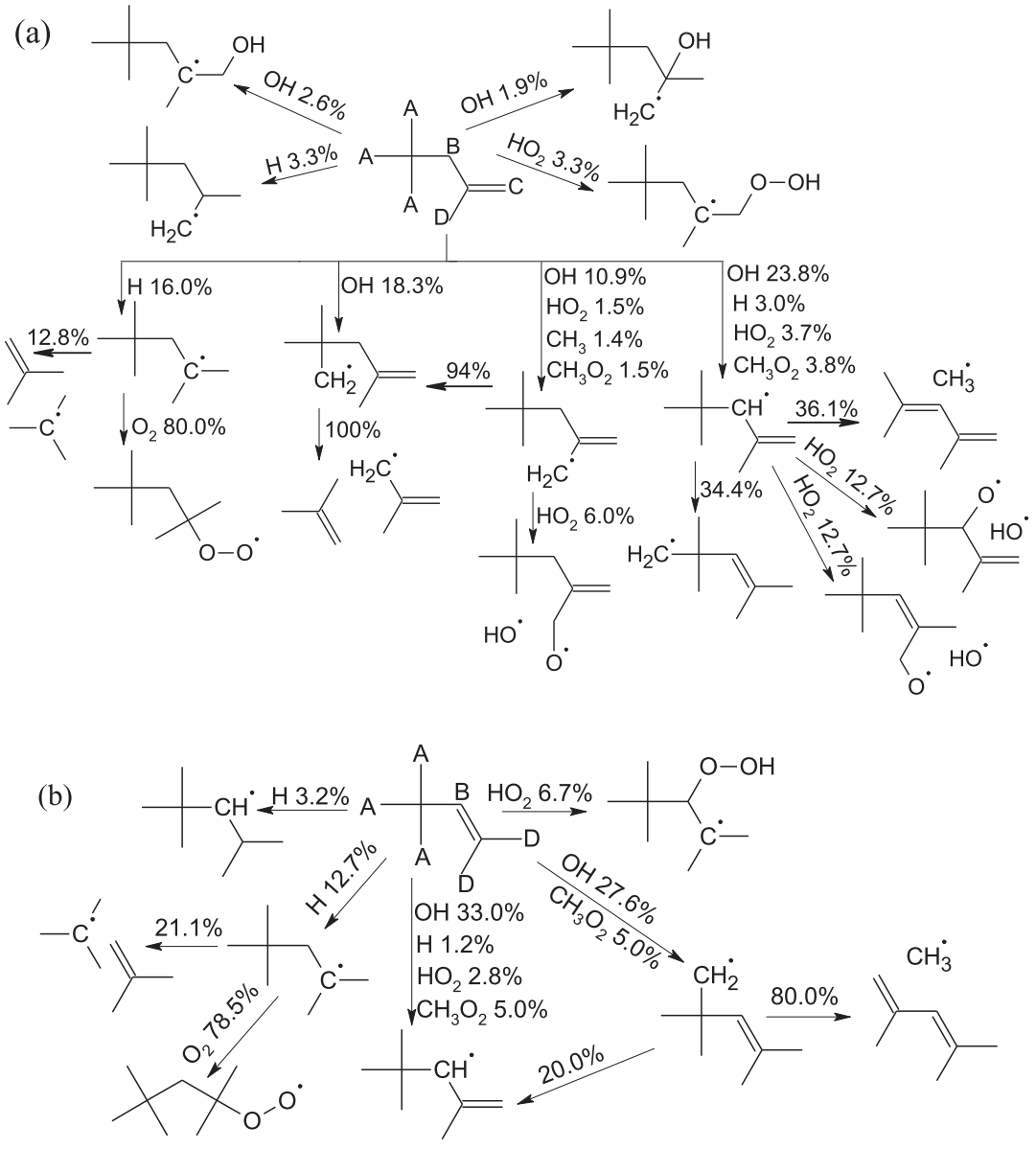

Fig. 11. Reaction flux analysis of (a) DIB-1 and (b) DIB-2 at fuel consumption rate of 20%, 30 bar, 800 K.

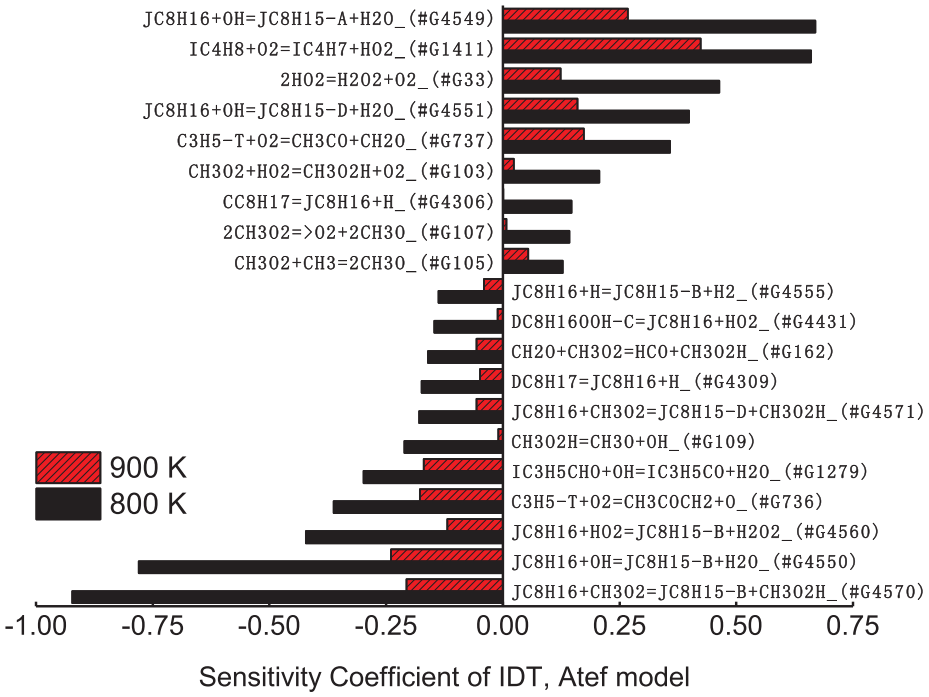

Fig. 12. Sensitivity analyses for stoichiometric DIB-1 mixture at 30 bar, 800 and 900 K.

which are respectively 35.8% and 57.5%. The frequency of the isomerization through 8-member ring transition state at the D sites is very low that this channel can be neglected even though it has a low energy barrier.

A great amount of DIB isomers are formed in the consumption channels shown in Fig. 9(b), (c), indicating that the DIB chemistry is also important to the *iso*-octane oxidation. Specially, the channel of O_2 addition on CC_8H_{17} eventually lead to a large percentage of DIB-1 or DIB-2 by eliminating HO_2 radicals.

The reaction flux analyses of DIB isomers at fuel consumption rate of 20%, 30 bar and 800 K are shown in Fig. 10. Distinct from the oxidation of *iso*-octane, additions of the H, OH and HO_2 radicals contribute a lot to the DIB consumption. The fuel derived radicals generated from the H-abstractions are mainly consumed by unimolecular decomposition while the O_2 addition reactions are missing in the present model.

For the DIB isomers, however, O_2 addition and the following isomerization reactions should be quite limited because the vinylic H atoms are very hard to be abstracted. Moreover, the double bond will also increase the rigid of a molecular making the frequency even lower for the transition state that involves a double bond. Therefore, for DIB-1, the peroxy radical added at the A site should mainly abstract H atoms from the other two A sites and B site; C-OO bond at the B (secondary allylic) or D site (primary allylic) is easy to be broken because of the low BDE and dissociate back to the reactants [43]. For DIB-2, the peroxy radical added at the A site mainly abstract H atoms from the other two A sites. IC_8H_{15}-D and JC_8H_{15}-B are resonant structures, and thus the reactions of O_2 addition on IC_8H_{15}-D are the same with that on JC_8H_{15}-B.

Sensitivity analyses were conducted for stoichiometric DIB-1 mixture at 30 bar, 800 and 900 K, as shown in Fig. 11. The sensitivity coefficient for each reaction was calculated using the following equation (presented in Fig. 12):

$$\text{Sensitivity coefficient} = (\tau_2 - \tau_{0.5})/\tau$$

where τ_2 and $\tau_{0.5}$ are respectively the IDTs computed with the rate constant increased or decreased by a factor of 2 of each one reaction. Noting that large perturbation in the sensitivity analysis might induce non-linear effects, smaller perturbation has been tested and gives the same results. A positive sensitivity coefficient indicates that this specific reaction increases the IDT, and thus decreases the system reactivity, and vice versa.

The most reactivity enhancing reactions are the H-abstractions forming JC_8H_{15}-B, because JC_8H_{15}-B can further add HO_2 on B or D site and generate OH radicals, as shown in Fig. 10(a). H-abstraction by OH radical from the A site forming JC_8H_{15}-A is the most reactivity inhibited reaction, because it consumes reactive OH radicals and further generates two stabilized products: IC_4H_8 and IC_4H_7-I_1. The H-abstraction on IC_4H_8 also shows relatively large sensitivity especially at high temperatures since a lot of IC_4H_8 are produced through β-scissions in the DIB-1 oxidation.

DIB isomers are important intermediates in the oxidation of *iso*-octane, however, typical low-temperature reactions are missing in the current DIB sub-mechanisms. Although these reactions do not show as much influence as that for linear alkenes, completing their reaction schemes will improve the model predictions at low temperatures and benefit the understanding of *iso*-octane kinetics. Also noting that IC_4H_8, IC_4H_{10} and their derived radicals are produced through many reaction pathways of *iso*-octane and DIB isomers, accurately describing the sub-models of IC_4H_8, IC_4H_{10} is also essential to the development of DIB and *iso*-octane models. However, the state-of-the-art features of IC_4H_8 and IC_4H_{10} kinetics are not included in the Atef model, therefore, further optimizations and validations of IC_4H_8 and IC_4H_{10} sub-models should be also conducted in the future works.

4. Conclusions

In this work, we have provided the IDTs of DIB-1, DIB-2, DIB blend and *iso*-octane at various equivalence ratios, high pressures and low to intermediate temperatures. DIB isomers did not show NTC nor two staged ignition behaviors and the reactivity of their blend is generally proportional to the concentration of each isomer.

Direct comparison on the IDTs of DIB-1, DIB-2 and *iso*-octane has reflected the effects of double bond and its position on the reactivities of branched alkenes. Similar to the large linear alkenes, inducing a double bond will decrease the reactivities at low temperatures while increase the reactivities at high temperatures compared with their

saturated structures. However, the effect of double bond position on the reactivities of DIB isomers has shown a different pattern with linear alkenes: DIB-2 shows higher reactivity than DIB-1 from low to high temperatures.

Experimental data measured in the present study has been used in the validations of kinetic models from the literature. Results show that the autoignitions of *iso*-octane can be well predicted by the current models, while the model predictions for DIB-1 still need to be improved especially at low temperatures. Further model development should work on completing the low-temperature reactions of DIB isomers and updating the IC_4H_8 and IC_4H_{10} sub-models.

CRediT authorship contribution statement

Yingtao Wu: Conceptualization, Data curation, Formal analysis, Methodology, Visualization, Writing - original draft. **Meng Yang:** . **Xiaoxin Yao:** . **Yang Liu:** . **Chenglong Tang:** Conceptualization, Formal analysis, Funding acquisition, Investigation, Methodology, Project administration, Resources, Supervision, Validation, Visualization, Writing - review & editing.

Declaration of Competing Interest

The authors declare that they have no known competing financial interests or personal relationships that could have appeared to influence the work reported in this paper.

Acknowledgements

This work is supported by the National Natural Science Foundation of China (51722603, and 91541107), CT is a TANG scholar and he appreciates the support from the Foundation of the National Defense Key Laboratory of Science and Technology on Combustion and Explosives. Yingtao Wu would like to thank the financial support from the China Scholarship Council (No. 201806280105).

Appendix A. Supplementary data

Supplementary data to this article can be found online at https://doi.org/10.1016/j.fuel.2020.118008.

References

[1] Pitz WJ, Mueller CJ. Recent progress in the development of diesel surrogate fuels. Prog Energy Combust Sci 2011;37(3):330–50.
[2] Mehl M, Pitz WJ, Westbrook CK, Curran HJ. Kinetic modeling of gasoline surrogate components and mixtures under engine conditions. Proc Combust Inst 2011;33:193–200.
[3] Kukkadapu G, Kumar K, Sung C-J, Mehl M, Pitz WJ. Autoignition of gasoline and its surrogates in a rapid compression machine. Proc Combust Inst 2013;34:345–52.
[4] Westbrook CK, Pitz WJ, Mehl M, Curran HJ. Detailed chemical kinetic reaction mechanisms for primary reference fuels for diesel cetane number and spark-ignition octane number. Proc Combust Inst 2011;33:185–92.
[5] Zhang K, Banyon C, Bugler J, Curran HJ, Rodriguez A, Herbinet O, et al. An updated experimental and kinetic modeling study of n-heptane oxidation. Combust Flame 2016;172:116–35.
[6] Atef N, Kukkadapu G, Mohamed SY, Al Rashidi M, Banyon C, Mehl M, et al. A comprehensive iso-octane combustion model with improved thermochemistry and chemical kinetics. Combust Flame 2017;178:111–34.
[7] Bugler J, Marks B, Mathieu O, Archuleta R, Camou A, Gregoire C, et al. An ignition delay time and chemical kinetic modeling study of the pentane isomers. Combust Flame 2016;163:138–56.
[8] Westbrook CK, Pitz WJ, Boercker JE, Curran HJ, Griffiths JF, Mohamed C, et al. Detailed chemical kinetic reaction mechanisms for autoignition of isomers of heptane under rapid compression. Proc Combust Inst 2002;29:1311–8.
[9] Curran HJ, Gaffuri P, Pitz WJ, Westbrook CK. A comprehensive modeling study of iso-octane oxidation. Combust Flame 2002;129(3):253–80.
[10] Andrae JCG, Brinck T, Kalghatgi GT. HCCI experiments with toluene reference fuels modeled by a semidetailed chemical kinetic model. Combust Flame 2008;155(4):696–712.
[11] Ra Y, Reitz RD. A combustion model for IC engine combustion simulations with multi-component fuels. Combust Flame 2011;158(1):69–90.
[12] Fikri M, Herzler J, Starke R, Schulz C, Roth P, Kalghatgi GT. Autoignition of gasoline surrogates mixtures at intermediate temperatures and high pressures. Combust Flame 2008;152(1–2):276–81.
[13] Mehl M, Faravelli T, Ranzi E, Lucchini T, Onorati A, Giavazzi F, et al. Kinetic modeling of knock properties in internal combustion engines. SAE technical paper. 2006. 2006-01-3239.
[14] Metcalfe WK, Pitz WJ, Curran HJ, Simmie JM, Westbrook CK. The development of a detailed chemical kinetic mechanism for diisobutylene and comparison to shock tube ignition times. Proc Combust Inst 2007;31:377–84.
[15] Mittal G, Sung C-J. Homogeneous charge compression ignition of binary fuel blends. Combust Flame 2008;155(3):431–9.
[16] Hu E, Yin G, Gao Z, Liu Y, Ku J, Huang Z. Experimental and kinetic modeling study on 2,4,4-trimethyl-1-pentene ignition behind reflected shock waves. Fuel 2017;195:97–104.
[17] Hu E, Yin G, Ku J, Gao Z, Huang Z. Experimental and kinetic study of 2,4,4-trimethyl-1-pentene and iso-octane in laminar flames. Proc Combust Inst 2019;37(2):1709–16.
[18] Yin G, Gao Z, Hu E, Xu Z, Huang Z. Comprehensive experimental and kinetic study of 2,4,4-trimethyl-1-pentene oxidation. Combust Flame 2019;208:246–61.
[19] Yin G, Hu E, Yang F, Ku J, Huang Z. Kinetics of H abstraction and addition reactions of 2,4,4-trimethyl-1-pentene by OH radical. Fuel 2017;210:646–58.
[20] Wang YK, Qin Y, Deng XY, Huang X. The investigation on non-linear characteristic of yawing moment of twin-tailed configuration. Proc Eng 2013;67:347–56.
[21] Zhong B-J, Zheng D. A chemical mechanism for ignition and oxidation of multi-component gasoline surrogate fuels. Fuel 2014;128:458–66.
[22] Li H, Qiu Y, Wu Z, Wang S, Lu X, Huang Z. Ignition delay of diisobutylene-containing multicomponent gasoline surrogates: shock tube measurements and modeling study. Fuel 2019;235:1387–99.
[23] Cancino LR, Fikri M, Oliveira AAM, Schulz C. Autoignition of gasoline surrogate mixtures at intermediate temperatures and high pressures: experimental and numerical approaches. Proc Combust Inst 2009;32(1):501–8.
[24] Ren S, Kokjohn SL, Wang Z, Liu H, Wang B, Wang J. A multi-component wide distillation fuel (covering gasoline, jet fuel and diesel fuel) mechanism for combustion and PAH prediction. Fuel 2017;208:447–68.
[25] Wu Y, Liu Y, Tang C, Huang Z. Ignition delay times measurement and kinetic modeling studies of 1-heptene, 2-heptene and n-heptane at low to intermediate temperatures by using a rapid compression machine. Combust Flame 2018;197:30–40.
[26] Vanhove G, Ribaucour M, Minetti R. On the influence of the position of the double bond on the low-temperature chemistry of hexenes. Proc Combust Inst 2005;30(1):1065–72.
[27] Wu Y, Yang M, Tang C, Liu Y, Zhang P, Huang Z. Promoting, “adiabatic core” approximation in a rapid compression machine by an optimized creviced piston design. Fuel 2019;251:328–40.
[28] Hu H, Keck J. Autoignition of adiabatically compressed combustible gas mixtures. SAE technical paper. 1987. 872110.
[29] Mehl M, Curran HJ, Pitz W, Westbrook CK. Chemical kinetic modeling of component mixtures relevant to gasoline. European combustion meeting, Vienna, Austria. 2009.
[30] Mehl M, Pitz WJ, Sjöberg M, Dec JE. Detailed kinetic modeling of low-temperature heat release for PRF fuels in an HCCI engine. Powertrains, fuels and lubricants meeting. 2009. p. 318–23.
[31] Benson SW. Thermochemical kinetics. 2nd ed. New York: Wiley; 1976.
[32] Weber BW, Sung CJ, Renfro MW. On the uncertainty of temperature estimation in a rapid compression machine. Combust Flame 2015;162(6):2518–28.
[33] Goldsborough SS, Hochgreb S, Vanhove G, Wooldridge MS, Curran HJ, Sung CJ. Advances in rapid compression machine studies of low- and intermediate-temperature autoignition phenomena. Prog Energy Combust Sci 2017;63:1–78.
[34] Wang Z, Qi Y, He X, Wang J, Shuai S, Law CK. Analysis of pre-ignition to super-knock: hotspot-induced deflagration to detonation. Fuel 2015;144:222–7.
[35] ANSYS CHEMKIN® academic research, release 18.2. ANSYS, Inc.
[36] Sarathy SM, Park S, Weber BW, Wang W, Veloo PS, Davis AC, et al. A comprehensive experimental and modeling study of iso-pentanol combustion. Combust Flame 2013;160(12):2712–28.
[37] Weber BW, Sung C-J. Comparative autoignition trends in butanol isomers at elevated pressure. Energy Fuels 2013;27(3):1688–98.
[38] Zhou C-W, Li Y, O'Connor E, Somers KP, Thion S, Keesee C, et al. A comprehensive experimental and modeling study of isobutene oxidation. Combust Flame 2016;167:353–79.
[39] Mehl M, Pitz WJ, Westbrook CK, Curran HJ. Kinetic modeling of gasoline surrogate components and mixtures under engine conditions. Proc Combust Inst 2011;33(1):193–200.
[40] Mehl M, Vanhove G, Pitz WJ, Ranzi E. Oxidation and combustion of the n-hexene isomers: a wide range kinetic modeling study. Combust Flame 2008;155(4):756–72.
[41] Barnard JA, Harwood BA. Slow combustion and cool-flame behavior of iso-octane. Combust Flame 1973;21(3):345–55.
[42] Curran HJ, Gaffuri P, Pitz WJ, Westbrook CK. A comprehensive modeling study of n -heptane oxidation. Combust Flame 1998;114(1–2):149–77.
[43] You X, Chi Y, He T. Theoretical analysis of the effect of CC double bonds on the low-temperature reactivity of alkenylperoxy radicals. J Phys Chem A 2016;120(30):5969–78.
[44] Mehl M, Pitz WJ, Westbrook CK, Yasunaga K, Conroy C, Curran HJ. Autoignition behavior of unsaturated hydrocarbons in the low and high temperature regions. Proc Combust Inst 2011;33(1):201–8.
[45] Yang F, Deng F, Zhang P, Hu E, Cheng Y, Huang Z. Comparative study on ignition characteristics of 1-hexene and 2-hexene behind reflected shock waves. Energy Fuels 2016;30(6):5130–7.